GENETICS

Cellular microRNA detection with miRacles: microRNA-activated conditional looping of engineered switches

Arun Richard Chandrasekaran[1]*, Molly MacIsaac[1,2*†], Paromita Dey[1], Oksana Levchenko[1,2], Lifeng Zhou[1], Madeline Andres[1‡], Bijan K. Dey[1,2§], Ken Halvorsen[1§]

MicroRNAs are short noncoding regulatory RNAs that are increasingly used as disease biomarkers. Detection of microRNAs can be arduous and expensive and often requires amplification, labeling, or radioactive probes. Here, we report a single-step, nonenzymatic microRNA detection assay using conformationally responsive DNA nanoswitches. Termed miRacles (microRNA-activated conditional looping of engineered switches), our assay has subattomole sensitivity and single-nucleotide specificity using an agarose gel electrophoresis readout. We detect cellular microRNAs from nanogram-scale RNA extracts of differentiating muscle cells and multiplex our detection for several microRNAs from one biological sample. We demonstrate 1-hour detection without expensive equipment or reagents, making this assay a compelling alternative to quantitative polymerase chain reaction and Northern blotting.

INTRODUCTION

MicroRNAs (miRNAs) are short, noncoding RNAs [18 to 25 nucleotides (nt)] that repress gene expression at the posttranscriptional level. They affect many biological processes, including cellular proliferation, differentiation, and apoptosis, leading to important consequences in normal development, physiology, and disease (*1*, *2*). Expression levels of individual miRNAs in tissues, cells, and bodily fluids can serve as stable biomarkers for cellular events or disease diagnosis (*3*, *4*), highlighting the importance of a simple and sensitive method for miRNA detection and quantification.

miRNA detection is challenging because of low abundance, small size, and sequence similarities. miRNAs comprise about 0.01% of total RNA (*5*), and individual miRNA levels range from a few copies to tens of thousands of copies per cell (*6*). Furthermore, miRNAs within a family can differ by a single nucleotide (*7*), and yet each specific miRNA can be differentially regulated during cellular processes or in disease conditions. Thus, miRNA detection strategies must be highly specific, able to correctly identify a few target molecules among an abundance of similar RNA molecules.

Traditional methods for detection of miRNAs include Northern blotting, quantitative reverse transcription polymerase chain reaction (qRT-PCR), next-generation sequencing, and microarray-based hybridization (*5*, *8*, *9*). Of these, only Northern blotting detects native miRNAs directly, while the others rely on additional labeling or amplification steps. These approaches can present substantial tradeoffs between cost, complexity, and performance. In addition, some of these methods require specialized equipment and/or skilled personnel and can involve complex and time-consuming procedures.

DNA nanotechnology has provided an alternative route to building devices and machines with desired applications (*10*) including biosensing (*11*). For miRNA detection, different groups have used DNA nanostructures in combination with nanoparticles (*12*, *13*), hybridization chain reaction (*14*, *15*), and transition-metal dichalcogenide nanosheets (*16*, *17*). More generally, in the DNA nanotechnology field, simple DNA-based devices have yielded practical applications, such as DNA-PAINT (DNA-based points accumulation for imaging in nanoscale topography) for three-dimensional imaging and quantification of proteins in situ (*18*–*19*), I-switch for pH detection (*20*–*21*), Clensor for quantifying chloride transport in cells (*22*), and nanoswitches for the detection of antibodies and proteins (*23*–*24*). As with those works, here, we show that a relatively simple DNA-based device can solve a complex biomedical challenge. Our assay, termed miRacles (microRNA-activated conditional looping of engineered switches), uses a "smart reagent" composed of rationally designed DNA nanoswitches to enable simple and low-cost detection of native miRNAs without specialized equipment (Fig. 1A).

The DNA nanoswitches were originally designed as tools for single-molecule biophysics experiments (*25*) and later recognized for their potential in quantitative analysis of biomolecular interactions using gel electrophoresis (*26*). Recent efforts in our laboratory and others have turned toward molecular detection, with Hansen *et al.* (*27*) demonstrating detection of proteins and our laboratory demonstrating proof-of-concept detection of synthetic DNA sequences (*28*). Here, we considerably expand upon that concept to develop a user-ready multiplexed method to detect and quantify miRNAs from nanogram-scale cellular RNA extracts in as little as an hour with common laboratory supplies.

RESULTS

The DNA nanoswitch in this work was designed as a linear duplex that forms a loop in the presence of a target miRNA (Fig. 1B and figs. S1 and S2). The nanoswitch was constructed using DNA origami approaches (*29*), formed by hybridizing short oligonucleotides (typically 60 nt) that are complementary to a single-stranded DNA (ssDNA) scaffold (7249 nt). Two distant "detector" strands (separated by ~2500 nt) were designed to contain overhangs complementary to different segments (typically halves) of the target miRNA. Recognition and binding of the miRNA reconfigure the switch from the linear "off" state to the looped "on" state. The two states can be quantified using standard agarose gel electrophoresis and gel stains,

[1]The RNA Institute, University at Albany, State University of New York, Albany, NY 12222, USA. [2]Department of Biological Sciences, University at Albany, State University of New York, Albany, NY 12222, USA.
*These authors contributed equally to this work.
†Present address: Program in Cellular and Molecular Medicine, Boston Children's Hospital, Boston, MA 02115, USA.
‡Present address: College of Agriculture and Life Sciences, Cornell University, Ithaca, NY 14853, USA.
§Corresponding author. Email: khalvorsen@albany.edu (K.H.); bdey@albany.edu (B.K.D.)

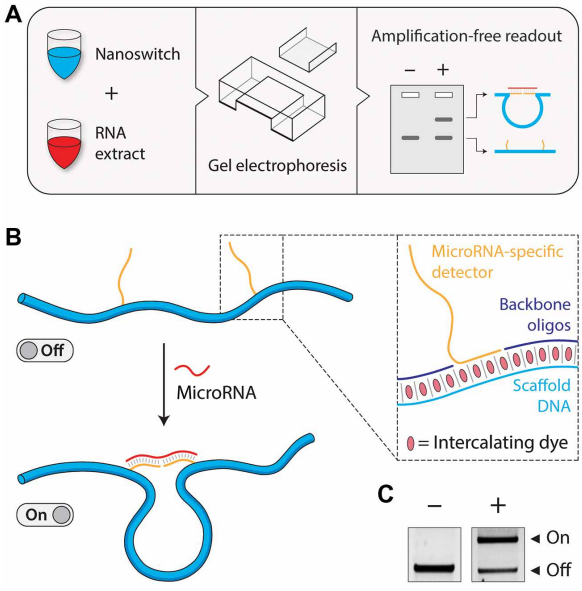

Fig. 1. Concept and workflow of the miRacles assay. (**A**) Workflow of the miRacles assay: Customized DNA nanoswitches are mixed with target miRNA sample, incubated, and run on an agarose gel for detection. (**B**) DNA nanoswitches undergo a conformational change from a linear "off" state to a looped "on" state when bound to a target miRNA. Inset: The nanoswitch is composed of a single-stranded M13 scaffold, backbone oligonucleotides, and single-stranded extensions (detectors) complementary to the target miRNA. Intercalating dyes intrinsic to the electrophoresis process provide the signal to visualize the nanoswitches. (**C**) The two conformations are resolvable in a standard agarose gel.

where the detection signal arises from the integrated intensity of the looped nanoswitch. Each nanoswitch recruits thousands of intercalating dye molecules [estimated at 1 dye for every 3.7 base pair (bp) for GelRed (*30*)] but has its fate (looped or unlooped) decided by a single miRNA, providing an inherent signal amplification. This compares favorably to a fluorescence resonance energy transfer (FRET) or quenched fluorescence output where each nanoswitch would only have a single (or a few) dye molecules.

For concept validation, we chose let-7b as a target miRNA because let-7b belongs to a highly conserved family of more than a dozen-related miRNAs varying by one or more nucleotides. These miRNAs have critical biological functions and are dysregulated in multiple human diseases (*31*). We customized DNA nanoswitches with detector strands that target the full sequence of let-7b and incubated them with synthetic let-7b miRNA. Running an agarose gel of the mixture, we showed that our DNA nanoswitches were capable of miRNA detection (Fig. 1C).

Next, we investigated the ability of our let-7b nanoswitches to distinguish closely related sequences, which occur naturally in some miRNAs. In previous work (*28*), we showed differential detection of two unrelated DNA oligos but did not establish selectivity among nearly matching sequences. Here, we tested our let-7b nanoswitches against either a synthetic let-7c target (1-nt mismatch) or a synthetic let-7a target (2-nt mismatch). Notably, our first results demonstrated single-nucleotide specificity, with a 1-nt mismatch between nanoswitch and target (let-7c), causing an 85% reduction in signal intensity compared to a perfect match (let-7b). A 2-nt mismatch (let-7a) completely abolished the signal (fig. S3A). Taking this initial result further, we aimed to completely eliminate the cross-talk signal between let-7b and let-7c. To achieve this, we rationally redesigned the nanoswitches to destabilize the interaction on the side containing the mismatch. By reducing the detector length on the appropriate strand by 3 nt, we demonstrate the effectiveness of this strategy to attain perfect specificity between these nearly identical miRNAs (Fig. 2A). Using DNA analogs, we further showed that let-7b nanoswitches do not cross-talk to six other members of the let-7 family (fig. S3B). To show a broader application beyond the let-7 family, we additionally validated specificity between three miRNA variants within the miR-15 family (fig. S4A). These results illustrate the high specificity of our assay, which has been a key challenge for miRNA detection (*8*, *9*).

The often low abundance of miRNAs requires high-sensitivity detection. For DNA oligos, we previously achieved a detection limit in the 10 pM/100 attomole (amol) range (*28*). To push this sensitivity further, we optimized our protocols to maximize the signal and minimize the background. By spiking our dye directly into the sample, choosing agarose with low background signal, and keeping our gels thin with smaller loading volumes, we were able to take long (45 to 60 s) exposures that enabled reliable detection for as low as ~0.2 amol for let-7b, corresponding to ~100,000 molecules (Fig. 2B and fig. S3C). We performed similar experiments for two other miRNAs (miR-15a and miR-206) and found levels of detection into subattomole to single-attomole range (fig. S4, B and C). We additionally measured the time course for detection of a low-concentration target (6 pM), which shows increasing signal until ~4 hours with little change beyond that time (Fig. 2C and fig. S3D). To expand the dynamic range, we used various incubation times to achieve miRNA detection spanning more than four orders of magnitude (Fig. 2D and fig. S3E), which closely mirrors the natural dynamic range of different miRNAs (*6*).

Moving beyond synthetic targets, we sought to establish the miRacles assay in cellular RNA extracts. Previous work from our laboratory and another has suggested that nanoswitch detection can be robust against biological "noise." These examples showed spike-in detection of DNA oligos amid random sequences or in diluted fetal bovine serum (FBS) (*28*) and spike-in detection of prostate-specific antigen in diluted FBS or diluted bovine urine (*27*). However, neither of these studies demonstrated detection of any molecules from actual biological samples, and to date, no published work has done so with this technology.

miRNAs are commonly studied in cell cultures, tissue samples, and body fluids, all of which can be readily processed to collect total RNAs (typically in microgram scale) and a small RNA subfraction (typically ~10% by mass). For this work, we used myoblast cells as a surrogate model system for muscle differentiation and miR-206 as our primary target. Among the first identified and most important miRNAs in differentiating skeletal muscle cells, miR-206 undergoes significant up-regulation, especially in late differentiation (*32*, *33*). We harvested undifferentiated and differentiated muscle cells and extracted total and small RNAs from these cells (Fig. 3A). We confirmed differentiation in these cells by Western blots (Fig. 3B) and immunocytochemistry (Fig. 3C) of early and late myogenic differentiation markers myogenin (Myog) and myosin heavy chain (MHC), respectively.

Individual miRNA species are commonly at the parts-per-million level by mass of total RNAs, illustrating the "needle in a haystack" type challenge faced in miRNA detection. To validate our assay for biological detection, we first started with the less complex small

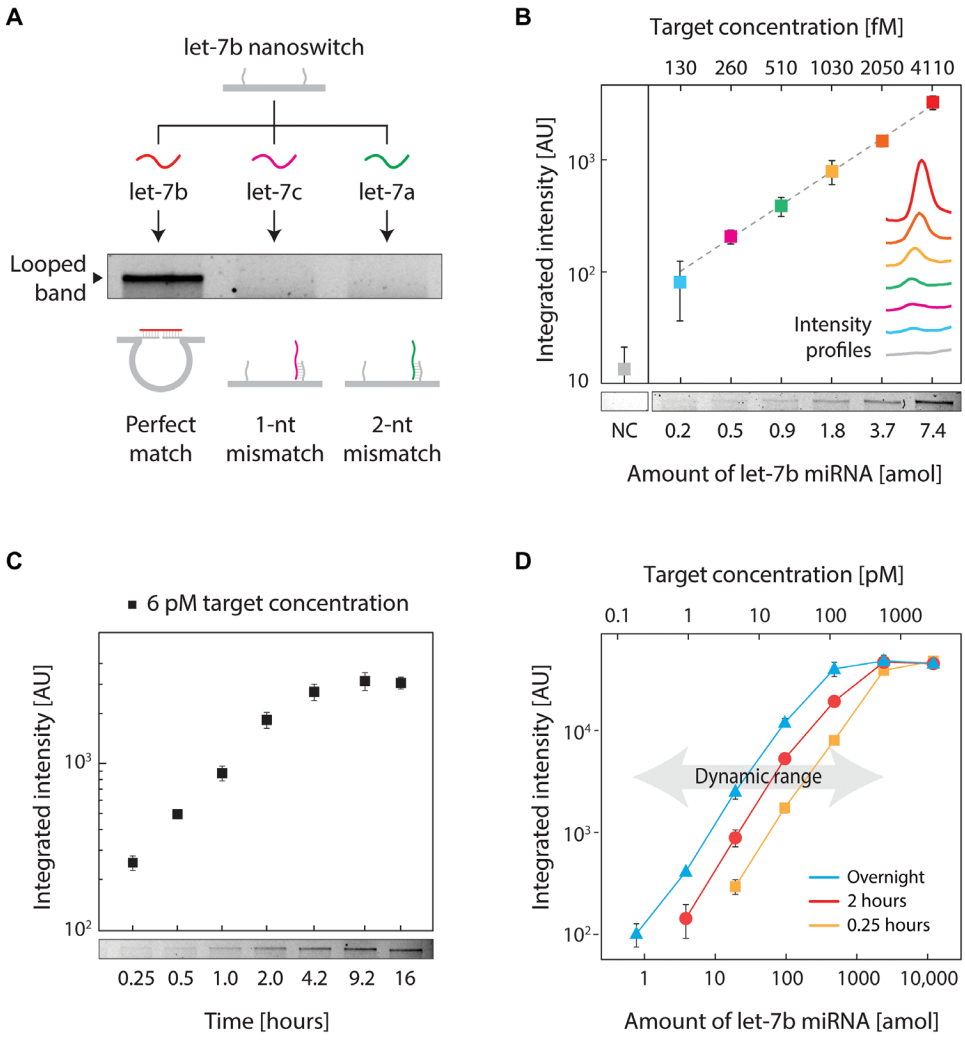

Fig. 2. Validation of the miRacles assay. (**A**) Specificity of the DNA nanoswitches with detectors designed for let-7b. As low as 1-nt mismatch between the detectors and the target miRNA eliminates the signal. (**B**) Limit of detection of the assay. NC, negative control. AU, arbitrary units. (**C**) Time course of the assay for a low-concentration target. (**D**) Dynamic range of the assay at different reaction times. Data points and error bars represent the means and SD, respectively, from triplicate measurements.

RNA subfraction. Using miR-206 targeting nanoswitches, we observed a progressive increase in miR-206 expression in small RNAs between undifferentiated samples and differentiation days 1 and 4 (Fig. 3, D and F). In particular, we found a 5.2-fold increase in miR-206 from growth medium (GM) to 1 day in differentiation medium (DM1) and a 62-fold increase from GM to 4 days in differentiation medium (DM4). We further showed that, by altering a single nucleotide on one of the detector strands, the detection signal was eliminated (fig. S5), validating the specificity within a biological context. In the less processed but more complex total RNA samples, prestaining the sample and annealing in a slow temperature ramp enabled miR-206 detection in 500 ng, with a similar trend to the small RNA fraction (Fig. 3, E and G and fig. S6). Here, we found a 5.5-fold increase from GM to DM1 and a 109-fold increase from GM to DM4.

In comparing our results with other miRNA methods, one author of this study has previously performed qRT-PCR and microarray experiments on miR-206 using total RNAs from the same cell type (*33*). All three methods show significant increases but with some variations in the amount of increase. The total miR-206 up-regulation determined from the miRacles assay (~109-fold) falls between the levels previously reported by qRT-PCR (~500-fold total) and microarray (~35-fold total). As an additional check, we retested our total RNA extract using qRT-PCR and found a 7.3-fold increase from GM to DM1 and a 75-fold increase from GM to DM4. These results indicate reasonable agreement between miRacles and other more established methods.

Focusing on the highly expressed miR-206 in the late differentiation samples (DM4), we were able to detect miR-206 in as little as 200 pg of small RNA and as little as 500 pg of total RNA (Fig. 3, H and I and fig. S7). Assuming ~20 pg of total RNAs per cell, this corresponds to only 25 cells. Assuming an attomole-level detection limit, these results would suggest that miR-206 is present in ~25,000 copies per cell in the DM4 samples, ~1200 copies per cell in DM1, and ~200 copies per cell in GM. To establish the broad applicability of our method for detecting cellular RNAs, we additionally probed for two miRNAs (let-7f and miR-16) in MCF-7, Jurkat, and A431 cell lines and detected expression of these miRNAs in all three cell lines (fig. S8).

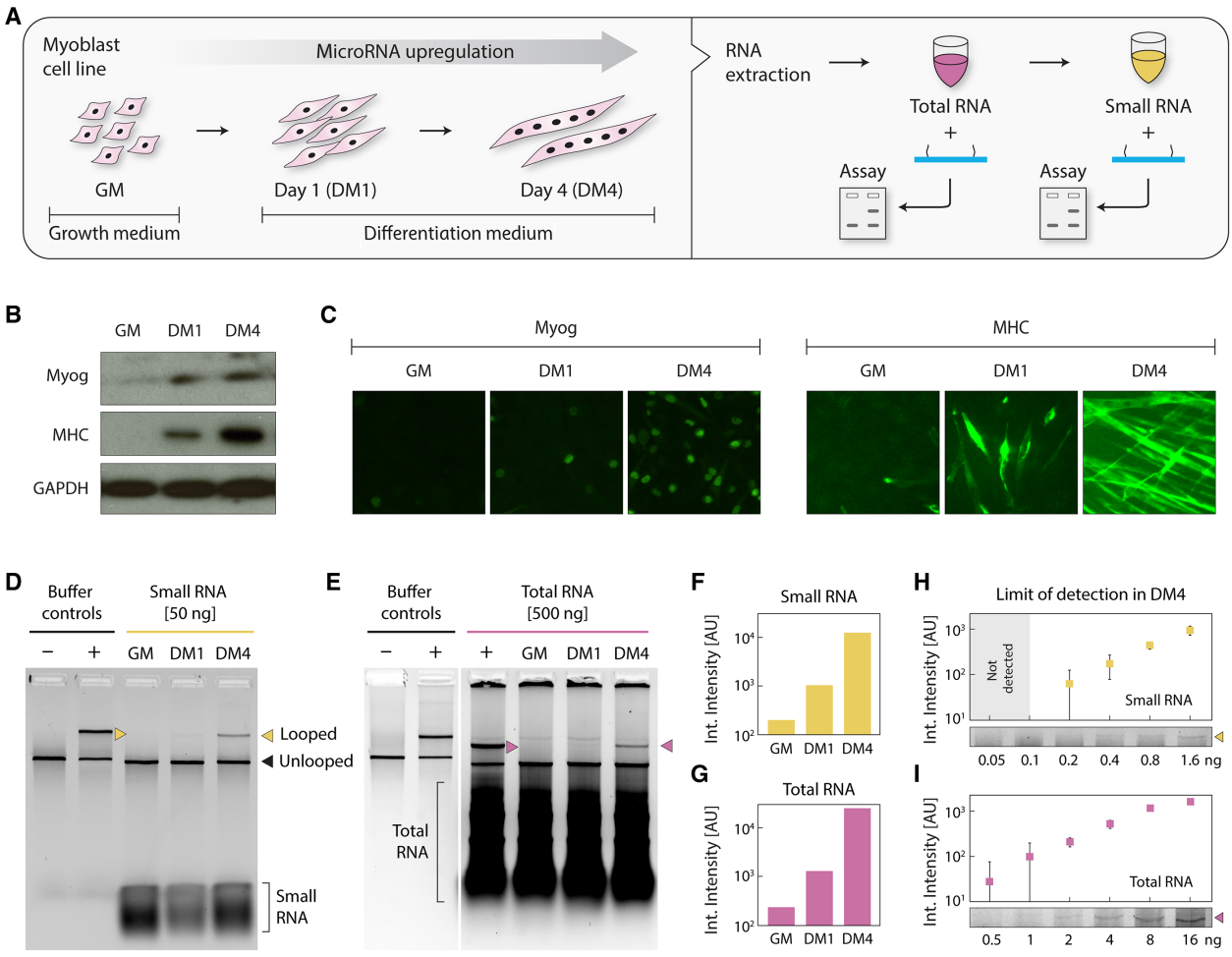

Fig. 3. miRNA detection from differentiating myoblast cells. (**A**) Schematic showing myoblast cells, harvested while growing in GM and on differentiation days 1 and 4, processed to yield total and small RNA fractions. An early myogenic differentiation marker, Myog, and a late myogenic differentiation marker, MHC, were measured by (**B**) Western blotting and (**C**) by immunocytochemistry to confirm differentiation. Both Myog and MHC were up-regulated in DM1 and DM4. GAPDH (glyceraldehyde-3-phosphate dehydrogenase) served as a control in (B). (**D**) We detected miR-206 in the differentiated samples with 50 ng of small RNAs and (**E**) with 500 ng of total RNAs. Quantification of gel intensities shows a sharp progressive up-regulation during differentiation, similar in both (**F**) small RNA and (**G**) total RNA samples. From DM4 samples, we note detection from as little as (**H**) 200 pg of small RNAs and (**I**) 500 pg of total RNAs. Error bars represent SD from triplicate measurements.

Often, multiple miRNAs alter their expression level during different cellular or disease stages. We used the programmability of the nanoswitches to develop a multiplexing system capable of detecting multiple miRNAs from the same sample. Detector strands can be placed at any desired locations on the DNA scaffold, resulting in loops of different sizes on binding the target miRNA. The loop size of the nanoswitch determines the gel migration, with each loop size showing as a unique band on the gel. We chose four miRNAs known to be present in these muscle cells (miR-206, miR-125b, miR-24, and miR-133-3p) and one negative control miRNA (miR-39) specific to *Caenorhabditis elegans*. We designed five individual nanoswitches with different loop sizes and combined them to form a multiplex system that produces a distinct band for each target sequence (Fig. 4A). In 50 ng of small RNAs, we detected the four miRNAs at various expression levels spanning nearly two orders of magnitude and confirmed no detection with the negative control (Fig. 4B). This multiplexing strategy enables direct comparison of miRNA levels in one sample without labeling or amplification and also moves a step in the direction of expanding the throughput of the miRacles assay.

DISCUSSION

Moving substantially from our proof-of-concept detection of synthetic DNA sequences (*28*), here, we have established, characterized, and optimized an miRNA detection assay that is ready for use with biological extracts. We emphasize that, while our group and others have previously demonstrated detection using DNA nanoswitches, this work represents the first example of detecting any biomolecule from a true biological sample.

Performance of the miRacles assay is competitive with commonly used techniques (table S1). Our selectivity of 1 nt has been difficult to achieve using other methods (*8*, *9*), and our sensitivity outperforms nonamplified methods including Northern blotting and microarray. While we cannot match the theoretical single-molecule sensitivity of qRT-PCR, in practice, this sensitivity is rarely achieved or required. Our 0.2 amol detection (~100,000 molecules) suggests that a 500-ng sample of total RNA (~25,000 cells) would enable detection of ~4 copies per cell. Given this low detection level, an increased sensitivity is not especially meaningful for most cellular extracts. Since our assay directly measures miRNAs without needing

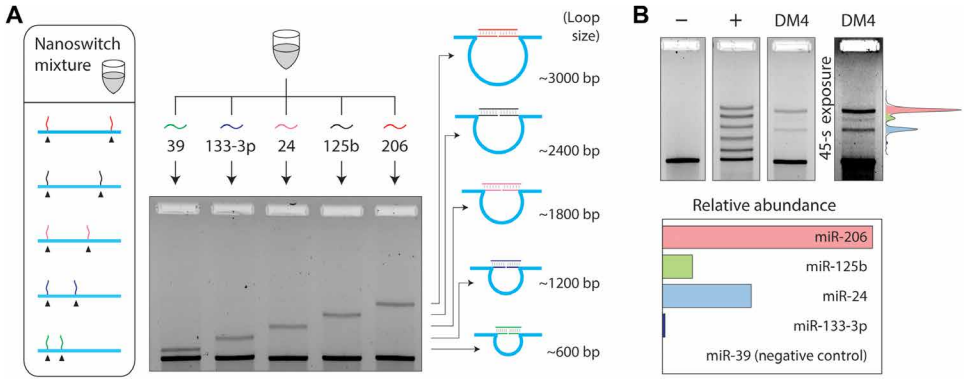

Fig. 4. Five-channel multiplexing. (**A**) Multiplexing enables the detection of different miRNAs with different loop sizes. (**B**) A multiplexed nanoswitch mixture shows five bands with similar intensity in a positive control consisting of all five target miRNAs. In 50 ng of DM4 small RNAs, four different miRNAs are detected at various expression levels, with miR-39 (a *C. elegans*–specific miRNA) not being detected.

amplification, protocols are simpler and avoid extra sample processing that can introduce errors.

Our assay also enables multiplexed quantitation of multiple native miRNAs from a single sample. Here, we have shown multiplexed detection of five miRNAs, and this capability could be expanded to accommodate more miRNAs. The primary limiting factors are resolving individual bands on the gel and the decrease in concentration of each miRNA sensing nanoswitch as more nanoswitches are added to the mix. Considering these limitations, we predict that multiplexed detection of 10 to 15 miRNAs could be achieved using this approach.

In stark contrast to other techniques, our minimalistic approach to miRNA detection is most notable for what is absent: There is no labeling, no amplification, no surface binding, no wash steps, no expensive equipment or reagents, and no complex protocols. Our DNA nanoswitches can be custom-made in advance at a relatively low cost and stored (wet or dry) for long-term use (fig. S9). Once made, simply mixing the nanoswitches with the sample liquid and running a gel produces high-quality results with common laboratory supplies. We illustrate this with a time-lapse video of start-to-finish miRNA detection from a biological sample in 1 hour (movie S1).

Our assay not only is immediately useful for measuring miRNAs from biological samples but also has potential for clinical applications. Detection of miRNA biomarkers (*3*, *4*) and biomarker panels (*34*) from bodily fluids is increasingly relevant for diagnosing and monitoring diseases. While detection of biological molecules from bodily fluids has not yet been established for DNA nanoswitches, some previous studies have shown promising results in detecting synthetic target molecules spiked into bovine serum or urine (*27*–*28*). Our study takes it one step closer to practical biosensing applications by demonstrating detection from biological samples. Scalable production with liquid handlers and liquid chromatography–based purification (*35*) could generate a complete library of miRNA nanoswitches, stored without refrigeration and used with minimal laboratory infrastructure. With these features in mind, we align with the broader concept of frugal science (*36*), a movement that has already produced clever low-cost solutions to blood centrifugation (*37*) and water purification (*38*), among others. As with those examples, we disrupt the typical cost/performance relationship, bringing simple miRNA detection to everyone's fingertips with mix-and-read smart reagents.

MATERIALS AND METHODS

Construction and purification of nanoswitches

Nanoswitches were constructed, as described previously (*26*, *28*). A cartoon outline of the construction protocol is shown in fig. S1, and the design of nanoswitch is shown in fig. S2. Briefly, a genomic ssDNA (New England BioLabs or Bayou Biolabs M13mp18) was linearized using targeted cleavage with BtsCI restriction enzyme. The linearized ssDNA was then mixed with a 10-fold molar excess of an oligonucleotide mixture containing the backbone oligonucleotides and detector oligonucleotides and was annealed from 90° to 20°C at 1°C min^{-1} in a T100 Thermal Cycler (Bio-Rad, USA). Oligonucleotides were purchased from Integrated DNA Technologies with standard desalting, and the full sequences of all strands are provided in the Supplementary Materials. Following construction, the nanoswitches were purified using ultrahigh-performance liquid chromatography (*35*) to remove excess oligonucleotides.

Cell culture and differentiation assay

Mouse myoblast cell line (C2C12) was acquired from the American Type Culture Collection. The cells were maintained at subconfluent densities in GM at 37°C in a tissue culture incubator with a constant supply of 5% CO_2. GM consists of Dulbecco's modified Eagle medium (DMEM; Gibco) supplemented with 10% FBS and 1× antibiotic-antimycotic (Life Technologies). For myogenic differentiation assay, the myoblast cells were grown to about 70% confluency, washed with phosphate-buffered saline (PBS), and cultured with DM. DM consists of DMEM containing 2% heat-inactivated horse serum (HyClone) and 1× antibiotic-antimycotic. Cells were harvested while growing in GM and after 24 and 96 hours (DM1 and DM4, respectively) in DM.

Total RNA extraction and small RNA isolation

Total RNAs were extracted using TRIzol reagent (Invitrogen) by following the manufacturer's instructions. Small RNAs were isolated from these total RNAs using a mirVana kit (Life Technologies). Total RNAs from MCF-7, Jurkat, and A431 cell lines were purchased from BioChain Inc.

Western blotting

Cells harvested either from GM or from different stages of DM were lysed in lysis buffer containing 50 mM tris-HCl, 150 mM NaCl, 0.1% NP-40, 5 mM EDTA, and 10% of glycerol supplemented

with protease inhibitor mix (Sigma-Aldrich). Cell lysates were centrifuged at 10,000 rpm for 5 min at 4°C to get rid of cell debris. Protein concentration was estimated by bicinchoninic acid assay (Pierce) using a plate reader. Proteins were separated in SDS–polyacrylamide gel electrophoresis, transferred, and immunoblotted with various antibodies. The antibodies used were mouse monoclonal antibody, anti-MHC, anti-GAPDH (glyceraldehyde-3-phosphate dehydrogenase; Sigma-Aldrich), and anti-Myog (Santa Cruz Biotechnology).

Immunocytochemistry

Cells of different stages were grown on a sterile glass coverslip and fixed with 2% formaldehyde in PBS for 15 min. Fixed cells were permeabilized with 0.2% Triton X-100 and 1% normal goat serum (NGS) in ice-cold PBS for 5 min. Then, cells were blocked with 1% NGS in PBS two times for 15 min each and incubated with primary antibody for 1 hour. Cells were washed three times with PBS and incubated with fluorescein isothiocyanate–conjugated antimouse immunoglobulin G (Dako) for 1 hour. After washing three times, the cells were mounted and imaging was carried out on an epifluorescence microscope (Olympus).

qRT-PCR for miRNAs

qRT-PCR for miRNAs was carried out by a miRCURY LNA RT kit (Qiagen) following the instructions of the manufacturer.

miRNA detection

In general, assays were performed by incubating the purified nanoswitches (~100 pM) with the target solution containing miRNAs. Concentration measurements were determined by measuring A_{260} absorbance with a NanoDrop spectrophotometer (Thermo Fisher Scientific) and applying either molar extinction coefficients (for oligos) or using the standard single-stranded RNA setting (for RNA extracts). Concentrations of final solutions were determined by the volume ratios during dilutions. Typical reactions were carried out in PCR tubes with 10-μl final volumes. Staining was performed by prestaining the samples with GelRed (Biotium Inc.) at 1× concentration and running a 25-ml (0.8%) agarose gel in 0.5× tris-borate EDTA at 75 V at room temperature for 45 min, unless otherwise noted. Specific protocol variations for each experiment are detailed as follows.

For the nanoswitch characterization tests, the target miRNAs were spiked into a 500 nM solution of off-target "blocking" oligos to minimize loss to the tubes. For the mismatch detection (Fig. 2A), the final concentration of target strands was 100 pM and the incubation time was 5 hours at room temperature in a solution containing nominally 1× PBS and 10 mM $MgCl_2$. For sensitivity tests (Fig. 2, B to D), microcentrifuge tubes and pipette tips were additionally preincubated in blocking oligo solution to minimize loss of the target miRNA. The nanoswitch and miRNA solution were incubated either overnight (Fig. 2B) or for various times (Fig. 2, C and D) at room temperature in a solution containing nominally 1× PBS and 10 mM $MgCl_2$. GelRed and a Ficoll-based loading dye were added to each sample to get a 1× concentration of each (for Fig. 2D, GelRed was added before incubation). Either 2.5 μl (Fig. 2, B and C) or 5 μl (Fig. 2D) of each sample was loaded and run in an unstained gel.

For detection of miRNAs from the small RNA samples (Fig. 3D), small RNAs were incubated with the nanoswitches overnight at room temperature in a solution containing nominally 1× PBS, 10 mM $MgCl_2$, and 1× GelRed. Ficoll-based loading dye was added to the samples before loading and running in an unstained gel. Detection from total RNAs (Fig. 3E) proceeded identically except without magnesium and with increased GelRed (3.3×) to prevent understaining with the high-added RNA content and incubated in a decreasing temperature ramp from 40° to 25°C with 5 min for each 0.1°C (total, ~12.5 hours). The limit-of-detection measurements in small and total RNAs (Fig. 3, H and I) proceeded similarly but with the addition of 500 nM blocking oligos to prevent loss to the tubes. In addition, both of those were incubated with magnesium but with GelRed added after incubation. For detection of other miRNAs from different cell lines, total RNA extracts were normalized to a concentration of 500 ng/μl.

For the multiplexed detection (Fig. 4), the five individual nanoswitches were concentration-normalized and mixed in equal volumes. Nanoswitches at ~100 pM each were mixed with small RNAs, 1× PBS, and 10 mM $MgCl_2$ and were incubated using the temperature ramp described above. GelRed and loading dye were added after incubation, and samples were run in an unstained gel. Gels were run at 4°C for 3 hours at 55 V, with the longer time facilitating easier recognition of the six individual bands.

Gel imaging and analysis

Imaging was done on a Bio-Rad Gel Doc XR+ imager using the default settings for GelRed with ultraviolet illumination. Images were typically taken at multiple exposures ranging from 5 to 45 s to facilitate accurate quantification. For each gel band, quantification was done using the highest-exposure image that did not contain saturated pixels in the band of interest (one exception—gel images for data shown in Fig. 2D required analysis of two partially saturated bands affecting two highest data points for the 15-min time). Thus, some gels were analyzed using multiple differently exposed images depending on the band brightness. These analyzed images were then normalized to the highest exposure. Nominally, this is done by scaling the ratio of the exposure times, but we additionally multiplied by a correction factor of 0.86 obtained by quantifying the same gel band across multiple identical images at different exposures. Efforts were made to take identical size images, but differently sized images could be normalized by the ratio of their pixel sizes. These normalizations only affected Fig. 2D, and the relative normalizations between small and total RNA are shown in Fig. 3, F and G.

To quantify each gel band, 12-bit images were imported into ImageJ and processed with a 2-pixel median filter to help reduce noise and small speckles and to eliminate hot pixels. Gel images were then rotated 90°, and a rectangular selection (of common size) was applied to each gel lane. In rare cases, where a bright speckle interfered with the band, we applied a smaller rectangle to analyze a fraction of the band. The plot profile command was used to get a mean intensity profile along the band width, and the area under the curve was quantified as a measure of the overall signal. While this analysis can also be done in ImageJ, we preferred to export the profiles to Origin 2017 (OriginLab) for a more precise quantification. In Origin, we used the peak analysis tool to draw a spline-interpolated baseline and measure the area between the profile and baseline. For the more complex multiplexing experiment, we instead explicitly subtracted the baseline using the same method and fit the subsequent profile with four Gaussian curves.

SUPPLEMENTARY MATERIALS

Supplementary material for this article is available at http://advances.sciencemag.org/cgi/content/full/5/3/eaau9443/DC1

Fig. S1. Design and construction of the DNA nanoswitch.
Fig. S2. Programmable design of the DNA nanoswitch.
Fig. S3. Concept validation using miRNA let-7b.
Fig. S4. Specificity and sensitivity in other miRNAs.
Fig. S5. Mismatch detection in small RNA samples.
Fig. S6. Protocol modification for total RNA detection.
Fig. S7. Sensitivity of miR-206 detection from RNA extracts.
Fig. S8. MicroRNA detection in different cell lines.
Fig. S9. Stability of the nanoswitch after drying.
Table S1. Comparison of miRacles assay with currently existing miRNA detection methods.
Movie S1. Time-lapse movie of miRNA detection in 1 hour using miRacles assay.

REFERENCES AND NOTES

1. M. S. Ebert, P. A. Sharp, Roles for microRNAs in conferring robustness to biological processes. *Cell* **149**, 515–524 (2012).
2. J. A. Vidigal, A. Ventura, The biological functions of miRNAs: Lessons from in vivo studies. *Trends Cell Biol.* **25**, 137–147 (2015).
3. M. A. Cortez, C. Bueso-Ramos, J. Ferdin, G. Lopez-Berestein, A. K. Sood, G. A. Calin, MicroRNAs in body fluids—The mix of hormones and biomarkers. *Nat. Rev. Clin. Oncol.* **8**, 467–477 (2011).
4. A. Allegra, A. Alonci, S. Campo, G. Penna, A. Petrungaro, D. Gerace, C. Musolino, Circulating microRNAs: New biomarkers in diagnosis, prognosis and treatment of cancer (Review). *Int. J. Oncol.* **41**, 1897–1912 (2012).
5. H. Dong, J. Lei, L. Ding, Y. Wen, H. Ju, X. Zhang, MicroRNA: Function, detection, and bioanalysis. *Chem. Rev.* **113**, 6207–6233 (2013).
6. D. P. Bartel, MicroRNAs: Genomics, biogenesis, mechanism, and function. *Cell* **116**, 281–297 (2004).
7. B. M. Ryan, A. I. Robles, C. C. Harris, Genetic variation in microRNA networks: The implications for cancer research. *Nat. Rev. Cancer* **10**, 389–402 (2010).
8. E. A. Hunt, D. Broyles, T. Head, S. K. Deo, MicroRNA detection: Current technology and research strategies. *Annu. Rev. Anal. Chem.* **8**, 217–237 (2015).
9. M. Baker, MicroRNA profiling: Separating signal from noise. *Nat. Methods* **7**, 687–692 (2010).
10. A. R. Chandrasekaran, N. Anderson, M. Kizer, K. Halvorsen, X. Wang, Beyond the fold: Emerging biological applications of DNA origami. *Chembiochem* **17**, 1081–1089 (2016).
11. A. R. Chandrasekaran, H. Wady, H. K. K. Subramanian, Nucleic acid nanostructures for chemical and biological sensing. *Small* **12**, 2689–2700 (2016).
12. X. Qu, D. Zhu, G. Yao, S. Su, J. Chao, H. Liu, X. Zuo, L. Wang, J. Shi, L. Wang, W. Huang, H. Pei, C. Fan, An exonuclease III-powered, on-particle stochastic DNA walker. *Angew. Chem. Int. Ed.* **56**, 1855–1858 (2017).
13. L. Qi, M. Xiao, X. Wang, C. Wang, L. Wang, S. Song, X. Qu, L. Li, J. Shi, H. Pei, DNA-encoded Raman-active anisotropic nanoparticles for microRNA detection. *Anal. Chem.* **89**, 9850–9856 (2017).
14. X. Qu, M. Xiao, F. Li, W. Lai, L. Li, Y. Zhou, C. Lin, Q. Li, Z. Ge, Y. Wen, H. Pei, G. Liu, Framework nucleic acid-mediated pull-down microRNA detection with hybridization chain reaction amplification. *ACS Appl. Bio Mater.* **1**, 859–864 (2018).
15. Z. Ge, M. Lin, P. Wang, H. Pei, J. Yan, J. Shi, Q. Huang, D. He, C. Fan, X. Zuo, Hybridization chain reaction amplification of microRNA detection with a tetrahedral DNA nanostructure-based electrochemical biosensor. *Anal. Chem.* **86**, 2124–2130 (2014).
16. M. Xiao, A. R. Chandrasekaran, W. Ji, F. Li, T. Man, C. Zhu, X. Shen, H. Pei, Q. Li, L. Li, Affinity-modulated molecular beacons on MoS_2 nanosheets for microRNA detection. *ACS Appl. Mater. Interfaces* **10**, 35794–35800 (2018).
17. M. Xiao, T. Man, C. Zhu, H. Pei, J. Shi, L. Li, X. Qu, X. Shen, J. Li, MoS_2 nanoprobe for microRNA quantification based on duplex-specific nuclease signal amplification. *ACS Appl. Mater. Interfaces* **10**, 7852–7858 (2018).
18. R. Jungmann, M. S. Avendaño, J. B. Woehrstein, M. Dai, W. M. Shih, P. Yin, Multiplexed 3D cellular super-resolution imaging with DNA-PAINT and Exchange-PAINT. *Nat. Methods* **11**, 313–318 (2014).
19. R. Jungmann, M. S. Avendaño, M. Dai, J. B. Woehrstein, S. S. Agasti, Z. Feiger, A. Rodal, P. Yin, Quantitative super-resolution imaging with qPAINT. *Nat. Methods* **13**, 439–442 (2016).
20. S. Modi, M. G. Swetha, D. Goswami, G. D. Gupta, S. Mayor, Y. Krishnan, A DNA nanomachine that maps spatial and temporal pH changes inside living cells. *Nat. Nanotechnol.* **4**, 325–330 (2009).
21. S. Surana, J. M. Bhat, S. P. Koushika, Y. Krishnan, An autonomous DNA nanomachine maps spatiotemporal pH changes in a multicellular living organism. *Nat. Commun.* **2**, 340 (2011).
22. S. Saha, V. Prakash, S. Halder, K. Chakraborty, Y. Krishnan, A pH-independent DNA nanodevice for quantifying chloride transport in organelles of living cells. *Nat. Nanotechnol.* **10**, 645–651 (2015).
23. S. Ranallo, M. Rossetti, K. W. Plaxco, A. Vallée-Bélisle, F. Ricci, A modular, DNA-based beacon for single-step fluorescence detection of antibodies and other proteins. *Angew. Chem. Int. Ed.* **54**, 13214–13218 (2015).
24. A. Porchetta, R. Ippodrino, B. Marini, A. Caruso, F. Caccuri, F. Ricci, Programmable nucleic acid nanoswitches for the rapid, single-step detection of antibodies in bodily fluids. *J. Am. Chem. Soc.* **140**, 947–953 (2018).
25. K. Halvorsen, D. Schaak, W. P. Wong, Nanoengineering a single-molecule mechanical switch using DNA self-assembly. *Nanotechnology* **22**, 494005 (2011).
26. M. A. Koussa, K. Halvorsen, A. Ward, W. P. Wong, DNA nanoswitches: A quantitative platform for gel-based biomolecular interaction analysis. *Nat. Methods* **12**, 123–126 (2015).
27. C. H. Hansen, D. Yang, M. A. Koussa, W. P. Wong, Nanoswitch-linked immunosorbent assay (NLISA) for fast, sensitive, and specific protein detection. *Proc. Natl. Acad. Sci. U.S.A.* **114**, 10367–10372 (2017).
28. A. R. Chandrasekaran, J. Zavala, K. Halvorsen, Programmable DNA nanoswitches for detection of nucleic acid sequences. *ACS Sens.* **1**, 120–123 (2015).
29. P. W. K. Rothemund, Folding DNA to create nanoscale shapes and patterns. *Nature* **440**, 297–302 (2006).
30. F. A. P. Crisafuli, E. B. Ramos, M. S. Rocha, Characterizing the interaction between DNA and GelRed fluorescent stain. *Eur. Biophys. J.* **44**, 1–7 (2015).
31. S. Roush, F. J. Slack, The let-7 family of microRNAs. *Trends Cell Biol.* **18**, 505–516 (2008).
32. J. Gagan, B. K. Dey, R. Layer, Z. Yan, A. Dutta, Notch3 and Mef2c proteins are mutually antagonistic via Mkp1 protein and miR-1/206 microRNAs in differentiating myoblasts. *J. Biol. Chem.* **287**, 40360–40370 (2012).
33. B. K. Dey, J. Gagan, A. Dutta, miR-206 and -486 induce myoblast differentiation by downregulating Pax7. *Mol. Cell. Biol.* **31**, 203–214 (2010).
34. W. Yuan, W. Tang, Y. Xie, S. Wang, Y. Chen, J. Qi, Y. Qiao, J. Ma, New combined microRNA and protein plasmatic biomarker panel for pancreatic cancer. *Oncotarget* **7**, 80033–80045 (2016).
35. K. Halvorsen, M. E. Kizer, X. Wang, A. R. Chandrasekaran, M. Basanta-Sanchez, Shear dependent LC purification of an engineered DNA nanoswitch and implications for DNA origami. *Anal. Chem.* **89**, 5673–5677 (2017).
36. G. Whitesides, "The frugal way: The promise of cost-conscious science," *The Economist: The World in 2012*, 17 November 2011, p. 154.
37. M. S. Bhamla, B. Benson, C. Chai, G. Katsikis, A. Johri, M. Prakash, Hand-powered ultralow-cost paper centrifuge. *Nat. Biomed. Eng.* **1**, 0009 (2017).
38. M. U. Sankar, S. Aigal, S. M. Maliyekkal, A. Chaudhary, A. A. Kumar, K. Chaudhari, T. Pradeep, Biopolymer-reinforced synthetic granular nanocomposites for affordable point-of-use water purification. *Proc. Natl. Acad. Sci. U.S.A.* **110**, 8459–8464 (2013).

Acknowledgments: We thank M. Belfort, P. Rangan, G. Fuchs, S. Ranganathan, and W. P. Wong for critical comments and suggestions on the manuscript. **Funding:** Research reported in this publication was supported by the NIH through NIGMS and NCI under awards R35GM124720 and R21CA212827, respectively, to K.H. and by the American Heart Association under award 17SDG33670339 to B.K.D. The content is solely the responsibility of the authors and does not necessarily represent the official views of the NIH or the American Heart Association. **Author contributions:** A.R.C., B.K.D., and K.H. designed the experiments. A.R.C., M.M., O.L., L.Z., M.A., and K.H. performed the nanoswitch experiments. P.D. and B.K.D. carried out the cell culture, myoblast differentiation, and total and small RNA extraction from these samples and performed Western blot and immunocytochemistry experiments. A.R.C., B.K.D., and K.H. wrote the manuscript, and all authors commented on and edited the manuscript. **Competing interests:** K.H. is an inventor on three patents/patent applications related to this work, filed by the President and Fellows of Harvard College and the Children's Medical Center Corporation (U.S. patent no. 9914958, issued 13 March 2018; U.S. patent application no. 20170369935, published 28 December 2017; and U.S. patent application no. 20180291434, published 11 October 2018). A.R.C. and K.H. are inventors on an additional patent application related to this work, filed by Children's Medical Center Corporation, the Research Foundation for The State University of New York, and the President and Fellows of Harvard College (U.S. patent application no. 20180223344, published 9 August 2018). A.R.C. is also an inventor on one additional patent application related to this work, originally filed by Confer Health Inc. (application no. WO2018119437A3, dated 19 July 2018), and a former employee of and has an equity interest in Confer Health Inc., a company that is developing point-of-care diagnostics. All other authors declare that they have no competing interests. **Data and materials availability:** All data needed to evaluate the conclusions in the paper are present in the paper and/or in the Supplementary Materials. Additional data related to this paper may be requested from the authors.

Submitted 2 August 2018
Accepted 29 January 2019
Published 13 March 2019
10.1126/sciadv.aau9443

Citation: A. R. Chandrasekaran, M. MacIsaac, P. Dey, O. Levchenko, L. Zhou, M. Andres, B. K. Dey, K. Halvorsen, Cellular microRNA detection with miRacles: microRNA-activated conditional looping of engineered switches. *Sci. Adv.* **5**, eaau9443 (2019).

ScienceAdvances

Cellular microRNA detection with miRacles: microRNA- activated conditional looping of engineered switches

Arun Richard Chandrasekaran, Molly MacIsaac, Paromita Dey, Oksana Levchenko, Lifeng Zhou, Madeline Andres, Bijan K. Dey and Ken Halvorsen

Sci Adv **5** (3), eaau9443.
DOI: 10.1126/sciadv.aau9443